Testing and Isolation Efficacy: Insights from a Simple Epidemic Model

February 23, 2021

1 Abstract

The effect of testing processes, including (testing and test reporting) on an epidemic dynamics (infection and recovery) can be studied at the individual level or the community level (e.g., nursing homes, LTC facilities, etc.). Gaining insights to determine the sensitivity of the epidemic dynamics with respect to the testing processes will depend on underlying factors including the level of focus (individual or community), assumptions (model), and the interplay between these factors. In particular, the fast test reporting may be beneficial at the community-level, supported by many studies, as it gives a rapid assessment of the situation, identifies hot spots, and may enable rapid contact-tracing. However, the potential advantage of a slow rate of test return on the dynamics of an epidemic is real, often neglected, and needs to be quantified. At the individual level, this advantage can manifest in the following sense: individuals awaiting their test results or who have tested positive may partially or fully self-isolate, thus reducing or eliminating their potential in the transmission process. In this paper, we investigated this individual-level effect of testing processes on the epidemic dynamics by developing a SIR-type model. Although the model development was motivated by the COVID-19 epidemic, the model has general epidemiological and testing structures. The realistic components of the model include testing intensity, test sensitivity and specificity, rate of test return, and isolation. The novel component is the compartment-specific relative testing weights, which reflect the testing strategies– surveillance, diagnosis, or control. Here, we showed that the slow test reporting can be beneficial on the dynamics of an epidemic. In particular, it is possible for the basic reproduction number, $\mathcal{R}_0$, to be increasing with respect to the rate of test return. Further, we compare two testing strategies, random vs. targeted, in this framework. We conclude that the targeted testing strategy is more effective than the random one in the sense that a lower range of testing intensity is required to keep $\mathcal{R}_0 < 1$. Also, targeted testing reduces the individual-level of advantage of a slow rate of test return.

2 Introduction

The observed dynamics of the COVID-19 epidemic are driven by both epidemiological processes (infection and recovery) and testing processes (testing and test reporting). In addi-

tion to shaping epidemic observations (via case reports), testing processes can also affect epidemiological dynamics. In particular, individuals who are awaiting the results of a test may partially or fully self-isolate, and individuals who have tested positive are more likely to self-isolate. We developed a model that incorporates mechanistic epidemic processes and testing in order to explore the effects of testing and isolation on epidemic dynamics.

Because individuals who have been tested or received a positive test are likely to self-isolate—reducing or eliminating their potentially infectious contacts—the dynamics of an epidemic will depend on who gets tested and why. For a given testing intensity (tests performed per day), testing will have a stronger effect on infection rates the more strongly it is focused on people who are infectious. This level of focus depends in turn on the purpose and design of testing programs. When testing is done for the purposes of disease surveillance (Foddai et al., 2020) we might expect tests to be assigned randomly across the population, thus we characterize it as *random* testing strategy. In an ideal world, some bias in selection for testing is probably inevitable, although a stratified sampling design would be preferred for statistical efficiency (Graubard and Korn, 1996) [**Ali:** *a better ref everyone?*].

Over the course of the COVID-19 pandemic, however, the vast majority of testing has been done with other goals – primarily diagnosis (determining the infection status for clinical purposes), or control (determining the infection status in order to quickly isolate cases that have been found by contact tracing), which we characterize as *targeted* testing strategies. In these cases, testing probabilities vary widely across epidemiological compartments; in our dynamical model, we will characterize these probabilities by assigning a *per capita* testing weight to each compartment that determines the *relative* probability that an individual in that compartment will be selected for testing (see Methods).

When testing is used primarily for diagnosis it will focus on people with infection-like symptoms; thus the testing weights for people with vs. without the infections will depend on the relative magnitudes of the probability of having the infection-like symptoms when infected. Specifically, for COVID-19 infection, the testing weights will depend on the relative proportions of presymptomatic or asymptomatic vs. symptomatic infections and the probability of having COVID-19-like symptoms when *not* infected (e.g., due to other respiratory illnesses). Testing for epidemic control will focus on people who are known to have been in contact with known infected cases; in this case the testing weights for infected vs. uninfected people will depend on the probability of infection given contact, as well as the thoroughness and effectiveness of the system for identifying suspicious contacts.

The main interest from the epidemiological point of view is to know whether the number of infected individuals goes through an exponential growth phase, following the introduction of an infection in a totally susciptable population, before the disease becomes extinct. This is determined by studying the basic reproduction number $\mathcal{R}_0$. It is defined as the expected number of secondary infections arising from a typical infective individual in a completely susceptible population (Dietz, 1993). In the early stages of an epidemic the number of infected individuals is expected to grow exponentially over time when $\mathcal{R}_0 > 1$, and to decline over time when $\mathcal{R}_0 < 1$. Although the value of $\mathcal{R}_0$ cannot completely characterize the dynamics of even the simplest epidemic model (Shaw and Kennedy, 2021), it does give a simple and widely accepted index for the difficulty of control, as well as some indication of the likely final size of an epidemic (Ma and Earn, 2006).

In order to understand the effect of testing processes on an epidemic dynamics, we deveo-

pled a mechanistic SIR-type model with epidemic and testing components. Here, we focus on the the effect of testing intensity, different levels of testing "focus" (from random to highly targeted), and rate of test return on the epidemic dynamics. Our model provides insights to the sensitivity of the epidemiological dynamics, through $\mathcal{R}_0$, with respect to the undelying epidemic and testing parameters. [**DJDE:** *This paragraph does not flow from the rest of the intro, and is a weird way to end when the point of the paper is about testing.*][**Ali:** *some edits/rewording are done, ok?*]

[**DJDE:** *There is some back and forth between generic discussion and COVID-19-specific comments. I think COVID should be used as motivation, but that the whole paper should be framed generically.*]

3 Methods

We developed a deterministic model, Eqs. (A1), which groups individuals based on disease status and testing status. Disease states include Susceptible, Infectious and Recovered (thus this is an SIR-type model), and testing status categorizes people as *untested*, waiting-for-*positive*, waiting-for-*negative*, or *confirmed positive* (Figure 1). Symbolically, the testing status of an individual in the disease compartment X, where $X \in \{S, I, R\}$, is reflected in the subscript, namely X_{u}, X_{p}, X_{n} and X_{c}, for *untested*, waiting-for-*positive*, waiting-for-*negative*, or *confirmed positive*, respectively. Further, two 'accumulator' compartments, N and P, were also incorporated in the model in order to collect cumulative reported negative or positive tests. The model and details of calculation of the basic reproduction number $\mathcal{R}_0$ are presented in the appendixs.

Table 1 defines the model parameters, which are generally straightforward *per capita* flows between compartments, or modifiers to these flow rates. The *per capita* testing intensity is defined as the number of daily tests taken in a population of size N_0. The novel component of the model comes in through the compartment-specific relative testing weights W_S, W_I and W_R; these give the relative rates at which people in the S, I, and R compartments are tested, respectively. For example, $W_I/W_S = 2$ means that infected individuals are tested at twice the *per capita* rate of susceptible individuals.

In order to link to more applied models, i.e., including both epidemiological and testing processes, we constructed this model so we could specify the total *per capita* testing rate. We do this by defining the weighted size of the testing pool $W = W_S S_{\mathrm{u}} + W_I I_{\mathrm{u}} + W_R R_{\mathrm{u}}$, and calculating a scaling parameter for testing as:

$$\sigma = \frac{\rho N_0}{W}. \tag{1}$$

Thus, the *per capita* testing rate for compartment X is $F_X = \sigma W_X$, where $X \in \{S, I, R\}$. For a high-sensitivity test, infected people typically flow through to the "confirmed positive" (I_{c}, R_{c}) compartments and are thus unavailable for further testing. Over the course of the epidemic, a fixed testing rate as specified in (1) can (if large enough) exhaust the pool of people available for testing, leading to a singularity when no one is left untested. Although this phenomenon does not affect our analysis of $\mathcal{R}_0$, it can affect the temporal dynamics (we discuss an adjustment to the model that solves this problem in the appendix).

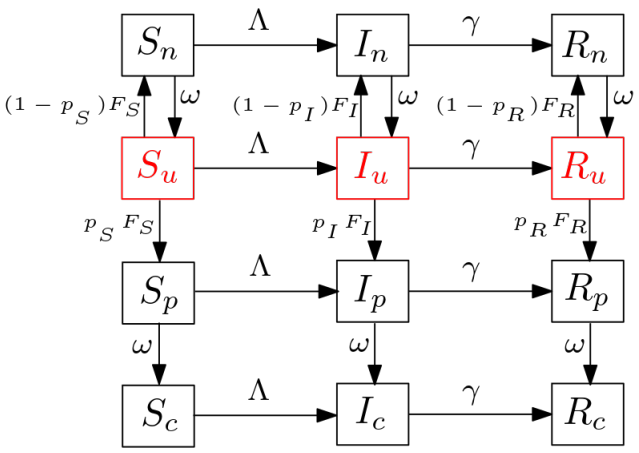

Figure 1: Flowchart of the SIR (Susceptible-Infectious-Recovered) model, A1. Here, the disease-based status of a compartment X, where $X \in \{S, I, R\}$, is combined with the testing-based status including $X_{\rm u}$, $X_{\rm p}$, $X_{\rm n}$ and $X_{\rm c}$, for *untested*, waiting-for-*positive*, waiting-for-*negative*, or *confirmed positive*, respectively. Also, Λ is the force of infection with definition in Eq. (2), γ is the recovery rate, ω is the rate of test return, F_X and p_X represent the *per capita* testing rate and the probability of positive tests, respectively, for compartment X. For further description of the parameters see Table 1. [**Ali:** *(i) will change the subs to roman font, (ii) not sure if ref color is helpful in u compartment?*]

The classical SIR model is based on the following implicit assumptions; well-mixed population, homogeneity of the population (i.e., all individuals are equaly susciptable and equaly infectious for the same length of time when infected), exponentially distributed duration of infection and large population size (see, e.g., Keeling and Rohani (2011)). In addition to these standard assumptions, our model, A1, assumes: (i) there is a single force of infection (new cases per unit time), Λ, defined as follows

$$\Lambda = \beta \frac{(I_{\rm u} + \eta_{\rm w} I_{\rm n} + \eta_{\rm w} I_{\rm p} + \eta_{\rm c} I_{\rm c})}{N_0}, \tag{2}$$

across all susceptible pools with transmission rate β and relative probability of transmission for "waiting" and *confirmed positive* individuals, $\eta_{\rm w}$ and $\eta_{\rm c}$ respectively, (see Table 1 for further details), (ii) $\eta_{\rm c} \leq \eta_{\rm w}$, i.e., the individuals awaiting test results have a higher transmission probability than the reported individuals. For this analysis, we also assume a perfectly specific test ($p_S = 0$). This last assumption combined with the assumption that no individual is in waiting-for-*positive* or *confirmed positive* compartments, i.e., $S_{\rm p}(0) = S_{\rm c}(0) = 0$, reduces the model to 10 equations (equations c and d in (A1) are eliminated).

The Disease-Free Equilibrium (DFE) for the SIR model, Eqs. (A1), is given by setting the differential equations to 0 and solving for the unknowns ([**Ali:** *is this clear or the "unkowns" needs to be defined? also * in sup for I and R?*]. The DFE is

$$S_{\rm n}^* = \frac{\rho}{\omega} N_0, \;\; S_{\rm u}^* = N_0 - S_{\rm n}^*, \;\; \text{and } I_j = R_j = 0 \text{ for all } j. \tag{3}$$

The basic reproduction number, $\mathcal{R}_0$, was calculated by using the next generation matrix

Symbol	Description	Unit	Value
N_0	Total population size	people	10^6
ω	Rate of onward flow from "waiting" to "confirmed" or "untested" compartments	1/day	-
γ	Recovery rate	1/day	1/3
ρ	Per capita testing intensity	1/day	0.01
η_{w}	Relative probability of transmission for "waiting" individuals	-	-
η_{c}	Relative probability of transmission for "confirmed positive" individuals	-	-
β	Transmission rate	1/day	0.39
Λ	Force of infection	1/day	-
p_S	Probability of positive tests for S $(= 1 - \text{specificity})$	-	0
p_I	Probability of positive tests for I $(= \text{sensitivity})$	-	1
p_R	Probability of positive tests for R $(= 1 - \text{specificity})$	-	0.5
W_S, W_I, W_R	Relative testing weights	-	Random: $\{1, 1, 1\}$ Targeted: $\{0.3, 1, 1\}$

Table 1: Parameters of the model (A1).

method developed by Van den Driessche and Watmough (2002). $\mathcal{R}_0$ is

$$\mathcal{R}_0 = \frac{\beta}{\gamma}(A \times S_{\mathrm{u}}^* + B \times S_{\mathrm{n}}^*) \times C, \tag{4}$$

where

$$\begin{aligned} A =& \gamma(\omega + \gamma) + (\gamma\eta_{\mathrm{w}} + \omega\eta_{\mathrm{c}}p_I)F_I, \\ B =& \big(\omega + (F_I + \gamma)\eta_{\mathrm{w}}\big)\gamma + \frac{(\eta_{\mathrm{w}}\gamma + \eta_{\mathrm{c}}\omega)\omega p_I F_I}{\omega + \gamma}, \\ C =& \frac{1}{N_0(\gamma(\omega + \gamma) + F_I(\gamma + \omega p_I))}. \end{aligned} \tag{5}$$

Further details of derivation of $\mathcal{R}_0$ are provided in the appendix section.

The analytical calculation of the next generation matrix and the derivation of $\mathcal{R}_0$ was carried out in Maple (Maplesoft, 2010) by using simple linear Algebra package. We used R (R Core Team, 2020) for the simulation part which included using the explicit expression of $\mathcal{R}_0$ 4 as a function of the underlying parameters, specifying the parameters a realistic range, calculating the corresponding $\mathcal{R}_0$ and plotting the contours of $\mathcal{R}_0$ (4). The related result is presented in Figure 2, where panel (2a) represents the random testing, and panel (2b) is representing non-random testing. The parameter values or ranges are presented in Table 1. This simulation reflects the behavior of $\mathcal{R}_0$ with respect to the selected parameters for two different testing strategies: (i) random testing, represented by all testing weights to be the same, $W_S = W_I = W_R$, and (ii) non-random testing, when testing weight are not equal. For simulation purposes we chose $W_S = W_I = W_R = 1$ for random testing, and $W_S = 0.3$ and $W_I = W_R = 1$ for non-random testing strategy. Note that the critical contour of $\mathcal{R}_0 = 1$ is plotted in solid line in Figure 2.

[**DJDE:** *Details such as the fact that you used ggplot are not important to state in the main text. On the other hand, there isn't a clear narrative here. The reader should feel that a story is being told.*][**Ali:** *addressed?, feedback is welcomed*]

4 Results

The explicit formula for the basic reproduction number, $\mathcal{R}_0$ (4), provides an opportunity to study the influence of changes in the underlying parameters on the critical index of epidemic dynamics. We are interested in understanding the effect of parameters that can be realistically controlled by changing in isolation, *per capita* testing intensity and test resulting, i.e., η_{c} and η_{w}, ρ and ω, respectively. The following Proposition is the direct result of taking partial derivative of $\mathcal{R}_0$ (4) with respect to selected parameters. Note that we used Taylor approximation of $\mathcal{R}_0$ at $\rho = 0$ due to the complexity of the expression and thus inconclusive.[**DJDE:** *in that case it would be good to establish numerically that the relationships given in the proposition are valid more generally, at least for reasonable parameter ranges*][**Ali:** *will do the simulation for testing intensity >> 1*] See the appendix for details.

[**DJDE:** *More importantly, you really need to state in words what this proposition is saying. The reader has to check the param table and think it through themselves.*]

Proposition 1. For model (A1), and by using the expression of the basic reproduction number $\mathcal{R}_0$ (4) ,

1. increasing the relative probabilities of transmission for tested individuals, increases $\mathcal{R}_0$;

$$\partial\mathcal{R}_0/\partial\eta_c \geq 0 \text{ and } \partial\mathcal{R}_0/\partial\eta_w \geq 0.$$

2. higher rate of testing reduces $\mathcal{R}_0$;

$$\partial\mathcal{R}_0/\partial\rho \leq 0 \text{ when } \rho \approx 0.$$

3. The rate of test return may result in the disease becomes extinct or not;

$$\partial\mathcal{R}_0/\partial\omega \text{ can be positive or negative when } \rho \approx 0.$$

Given that the perfect isolation occurs when no one transmits while waiting for test results (i.e., $\eta_c = \eta_w = 0$), Prop. 1 means that lifting the isolation from awaiting group results in an increased $\mathcal{R}_0$ and consequently a greater number of infected individuals. Prop. 2 indicates that increasing the *per capita* testing intensity, ρ, reduces $\mathcal{R}_0$. Lastly, Prop. 3 means that speeding up the test reporting may or may not reduce $\mathcal{R}_0$, it will depend on other parameters. It is straightforward to derive 2 and 3 from the Taylor approximation of $\mathcal{R}_0$ at $\rho = 0$. [**DJDE:** *can we gain some insight from the expressions for the partial derivatives in the proposition, as opposed to just their signs?*][**Ali:** *help*]

Our numerical solutions in support of the analytical results in Proposition 1 are presented in Figure 2. It can be inferred that when random testing strategy is applied, Figure 2a, comparing to the targeted testing strategy, Figure 2b, the critical *per capita* testing intensity of the corresponding panels are lower in non-random testing. Also, it appears that speeding the test reporting, i.e., increasing ω, does not significantly lower $\mathcal{R}_0$ when awaiting people (including people in I_p and I_n compartments) follow the isolation perfectly, i.e., η_w is closer to 0. However, speeding the test reporting reduces the epidemic more when the awaiting people less follow the isolation, i.e., η_w is closer to 1.

Furthermore, we derived an inequality that quantifies the exact relationships between model parameters that result in returning tests more rapidly being favorable (A16). [**DJDE:** *What do we learn from this inequality? Why is it relegated to an appendix?*]

5 Discussion

Mathematical modeling of infectious disease outbreaks provides insights on how testing processes influence the epidemiological processes through isolation. Here, we develop a compartmental SIR-type model to study the potential effect of testing strategies, testing intensity, test sensitivity and specificity, test reporting time and isolation on epidemic dynamics. While targeted testing strategies [**DJDE:** *you need to be clearer: you mean targeting individuals who have contacted people who were infected. For example, here you could say something like "While targeting the contacts of confirmed cases..."*] are always more effective than random testing, as expected, we find that in some cases the direct effect of testing is that viral

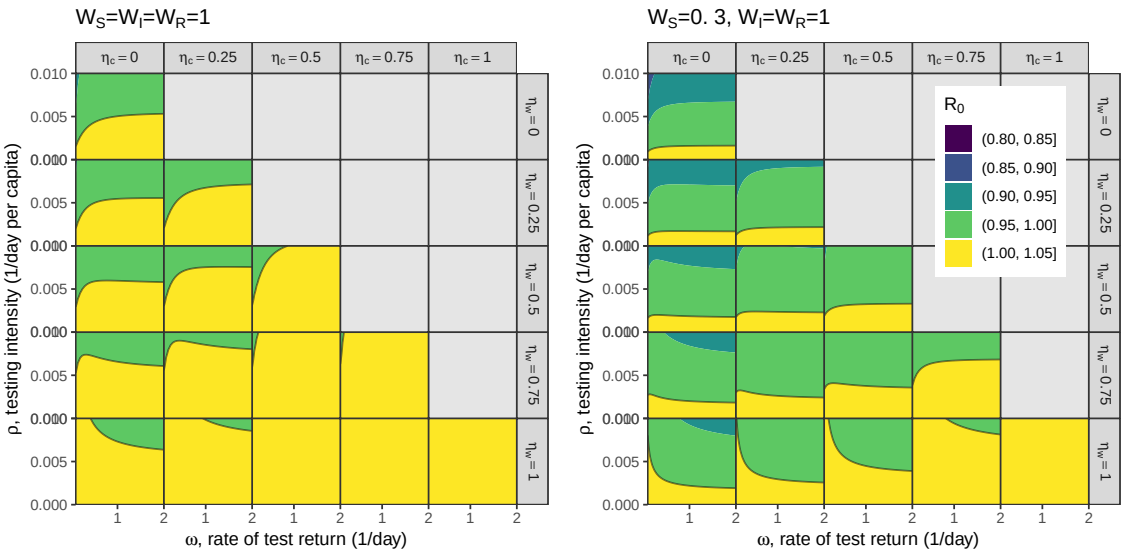

(a) (b)

Figure 2: **A comparison of the behaviour of the basic reproduction number, $\mathcal{R}_0$, between random versus targeted testing strategies at differnt levels of testing and isolation.** We numerically evaluate $\mathcal{R}_0$ (4) using the following parameters (listed in Table 1): $N_0 = 1 \times 10^6$, $\omega \in [0.1, 2]$ 1/day, $1/\gamma = 3$ days, $\rho \in [0, 0.01]$ 1/day, $\eta_{\rm w} \in [0, 1]$, $\eta_{\rm c} \in [0, 1]$, $\beta = 0.39$ 1/day, $p_S = 0$, $p_I = 1$ and $p_R = 0.5$. Contours of $\mathcal{R}_0$ are plotted for two testing strategies identified by a set of relative testing weights; (a) random testing where $W_S = W_I = W_R = 1$ and (b) targeted testing where $W_S = 0.3$ and $W_I = W_R = 1$. The black solid line in each panel represents the critical contour of $\mathcal{R}_0 = 1$. [**BMB:** *we still have some collisions in the y-axis tick labels*]

spread is greater for a slow test than for a fast test. This counter-intuitive effect can occur when people are cautious when awaiting a test result, and may not be robust to second-order effects of fast testing (such as better contact tracing).

We incorporated the compartment-specific relative testing weights, W_S, W_I and W_R, to model random testing and *targeted* testing strategies. Here, in the case of targeted testing and for the simplicity and illustration purposes, we assumed that infected and recovered individuals are tested at three times the *per capita* rate of susceptible individuals, thus $W_I/W_S = 3$ and $W_R = W_I$. Note that we have not specified a methodology to assign particular relative testing weights corresponding to a particular targeted testing scenario. This part needs to be developed further in future work. Modeling different targeted testing strategies, equivalently test-specific testing weights in our framework, requires prior information of the conditional probabilities of getting tested for people in a given compartment. This can be implied when we would like to quantify and compare the effect of different levels of test focus for infectious people on the basic reproduction number $\mathcal{R}_0$, and conclude about the disease spread management. For example, when people are tested for "screening", the individuals with potential higher mobility, eg. people who are getting on flights, get more tested and thus the coresponding heavier testing weight is assigned than people awaiting for a surgery and are probably going to stay in a long-term care facility and consequently less

mobile and more isolated to begin with. With our model, we would be able to compare the sensitivity of the disease dynamics, through $\mathcal{R}_0$, with respect to testing processes.

The *per capita* testing intensity, ρ; Proposition 1 part 2 and also Figure 2 indicates that increasing testing intensity ρ reduces $\mathcal{R}_0$. This is sensible since as people are moved to test compartments, namely X_p and X_n for $X \in \{S, I, R\}$, they may partially or fully self-isolate. Also individuals who have tested positive, namely X_c compartment for $X \in \{S, I, R\}$, are highly likely to self-isolate. The higher probability of being subject to isolation, the lower the force of infection (2) and the lower $\mathcal{R}_0$ will become. While our simulation supported this result, analytically it appeared to be hard to conclude this due to the complexity of $\mathcal{R}_0$ expression.

The potential advantage of slow test reporting, or favorable-delay-reporting; Individuals are highly likely to fully self-isolate when they are either awaiting the test results or they are reported, thus reducing or eliminating their potentially infectious contacts. Thus, the faster the test reporting rate, ω, the shorter these individuals stay in the "*safe*" awaiting-confirmed compartments, namely X_n, X_p and X_c for $X \in \{S, I, R\}$, and the more they get involved in the infection process. This advantage of slow test reporting is real, and neglected. We also compare to an individual-level advantage of fast tests: people who test positive may be even more careful. In our model analysis, Proposition 1 part 3 is describing this potential advantage. It states that returning test results more rapidly, i.e., increasing the rate ω, does not necessarily lower the reproduction number $\mathcal{R}_0$; whether increasing ω lowers $\mathcal{R}_0$ depends on the precise combination of model parameters including test reporting rate, testing strategies represented by compartment-specific testing weights, test sensitivity and specificity, and the level of isolation. Specifically, in the case of perfect isolation, i.e., when $\eta_{\mathrm{w}} = 0$ and $\eta_{\mathrm{c}} = 0$, $\mathcal{R}_0$ may increase as the test reporting process becomes faster. This can be seen from expression (A7). Another example of this favorable delay in ω could be when the test being employed produces many false negatives. Because many infected asymptomatic individuals will believe they are uninfected/uninfectious, thus may unknowingly spread the virus to many others. Again the delay in the test reporting rate keeps these individuals in the "*safe*" awaiting-confirmed compartments.

we are missing out on community-level advantages of fast testing: better assessment of the situation, identification of hot spots, contact-tracing, etc. The *per capita* testing intensity of CIVID-19 after about a year from the first case reported in December 2019, is still low ($(\rho \approx 0)$ in our model). In near future new test kits may be widely accessible, our model provide insights in this case. In particular, if a cheap test can identify on average more infected individuals as an expensive test, then our model predicts that the cheap test will lower $\mathcal{R}_0$ more. In contrast, if an expensive test can identify on average more infected individuals, it will not necessarily lower $\mathcal{R}_0$ more than the cheap test. The use of tests cheaper than RT-PCR has been proposed as a potential strategy for containing the COVID pandemic. While cheaper tests may be less sensitive and reliable than RT-PCR, they allow for broader and more intense testing. Using our Taylor approximation of $\mathcal{R}_0$ near $\rho = 0$, we examined what circumstances (i.e., model parameters) make the use of one test more favourable than another, and give a complete description through inequality A17. In general, we found that the expensive test tends to more effectively lower $\mathcal{R}_0$ when (a) individuals who test positive self-isolate much more than individuals who are waiting for their test result, (b) the time it takes to return tests is much shorter than the mean infectious period, and (c) the testing

intensity is much greater for infected individuals than susceptible individuals.

[**Ali:** *not sure if we want these 2 following parageraphs, or shrink it into afew short sentences?*] In addition to the favorable-delay-reporting observation of our model (A1), the model enables us to quantify the amount of delay required in the test reporting process as a strategy to reduce $\mathcal{R}_0$. To give a biological interpretation, we describe the qualitative trends predicted by the inequality (A16). To summarise, returning test results more rapidly tends to be favourable (i.e., reduces $\mathcal{R}_0$) when (i) *Confirmed-positive* individuals, lower their contact much more than individuals who are waiting for their test results (i.e., $\eta_c \ll \eta_w$), (ii) the test is highly sensitive (i.e., p_I is close to 1), and (iii) the targeted testing strategy is used (i.e., $W_i \gg W_s$).

one point we can make when discussing the relative weight of testing in different compartments is to discuss pre-testing screening tools, such as surveys or questionnaires. If we have a quantitative description of how the testing intensities affect the dynamics, we can make statements like "our results suggest that employing a pre-testing screening tool can help target infected individuals more effectively. In particular, doubling the sensitivity of the pre-screening tool would *do something* to $\mathcal{R}_0$.

[**DJDE:** *Some of this reads like notes for discussion rather than text for the paper, so I'm not trying to edit.*]

References

Arino, J. and Portet, S. (2020). A simple model for COVID-19. *Infectious Disease Modelling*.

Bergstrom, T., Bergstrom, C. T., and Li, H. (2020). Frequency and accuracy of proactive testing for COVID-19. *medRxiv*.

de Celles, M. D., Casalegno, J.-S., Lina, B., and Opatowski, L. (2020). Influenza may facilitate the spread of SARS-CoV-2. *medRxiv*.

Dietz, K. (1993). The estimation of the basic reproduction number for infectious diseases. *Statistical methods in medical research*, 2(1):23–41.

Elbanna, A., Wong, G. N., Weiner, Z. J., Wang, T., Zhang, H., Liu, Z., Tkachenko, A. V., Maslov, S., and Goldenfeld, N. (2020). Entry screening and multi-layer mitigation of COVID-19 cases for a safe university reopening. *medRxiv*.

Endo, A., Leclerc, Q. J., Knight, G. M., Medley, G. F., Atkins, K. E., Funk, S., Kucharski, A. J., et al. (2020). Implication of backward contact tracing in the presence of overdispersed transmission in COVID-19 outbreaks. *Wellcome Open Research*, 5(239):239.

Foddai, A., Lubroth, J., and Ellis-Iversen, J. (2020). Base protocol for real time active random surveillance of coronavirus disease (COVID-19)–adapting veterinary methodology to public health. *One Health*, page 100129.

Graubard, B. I. and Korn, E. L. (1996). Modelling the sampling design in the analysis of health surveys. *Statistical methods in medical research*, 5(3):263–281.

Jenness, S. M., Willebrand, K. S., Malik, A. A., Lopman, B. A., and Omer, S. B. (2020). Modeling dynamic network strategies for SARS-CoV-2 control on a cruise ship. *medRxiv*.

Keeling, M. J. and Rohani, P. (2011). *Modeling infectious diseases in humans and animals*. Princeton University Press.

Larremore, D. B., Wilder, B., Lester, E., Shehata, S., Burke, J. M., Hay, J. A., Tambe, M., Mina, M. J., and Parker, R. (2020). Test sensitivity is secondary to frequency and turnaround time for COVID-19 screening. *Science Advances*, page eabd5393.

Lopman, B., Liu, C., Le Guillou, A., Handel, A., Lash, T. L., Isakov, A., and Jenness, S. (2020). A model of COVID-19 transmission and control on university campuses. *medRxiv*.

Ma, J. and Earn, D. J. D. (2006). Generality of the final size formula for an epidemic of a newly invading infectious disease. *Bulletin of Mathematical Biology*, 68(3):679–702.

Maplesoft (2010). *Maple (14)*. a division of Waterloo Maple Inc., Waterloo, Ontario.

R Core Team (2020). *R: A Language and Environment for Statistical Computing*. R Foundation for Statistical Computing, Vienna, Austria.

Rice, K., Wynne, B., Martin, V., and Ackland, G. J. (2020). Effect of school closures on mortality from coronavirus disease 2019: old and new predictions. *BMJ*, 371.

Ruszkiewicz, D. M., Sanders, D., O'Brien, R., Hempel, F., Reed, M. J., Riepe, A. C., Bailie, K., Brodrick, E., Darnley, K., Ellerkmann, R., et al. (2020). Diagnosis of COVID-19 by analysis of breath with gas chromatography-ion mobility spectrometry: a feasibility study. *EClinicalMedicine*, page 100609.

Shaw, C. L. and Kennedy, D. A. (2021). What the reproductive number R0 can and cannot tell us about COVID-19 dynamics. *Theoretical Population Biology*.

Tuite, A. R., Fisman, D. N., and Greer, A. L. (2020). Mathematical modelling of COVID-19 transmission and mitigation strategies in the population of Ontario, Canada. *CMAJ*, 192(19):E497–E505.

Van den Driessche, P. and Watmough, J. (2002). Reproduction numbers and sub-threshold endemic equilibria for compartmental models of disease transmission. *Mathematical biosciences*, 180(1-2):29–48.

Appendix

5.1 Model and calculation of $\mathcal{R}_0$

The model in the form of a system of ordinary differential equations is

$$
\begin{aligned}
dS_{\mathrm{u}}/dt &= -\Lambda S_{\mathrm{u}} - F_S S_{\mathrm{u}} + \omega S_{\mathrm{n}}, && \text{(A1a)}\\
dS_{\mathrm{n}}/dt &= -\Lambda S_{\mathrm{n}} + (1-p_S) F_S S_{\mathrm{u}} - \omega S_{\mathrm{n}}, && \text{(A1b)}\\
dS_{\mathrm{p}}/dt &= -\Lambda S_{\mathrm{p}} + p_S F_S S_{\mathrm{u}} - \omega S_{\mathrm{p}}, && \text{(A1c)}\\
dS_{\mathrm{c}}/dt &= -\Lambda S_{\mathrm{c}} + \omega S_{\mathrm{p}}, && \text{(A1d)}\\
dI_{\mathrm{u}}/dt &= \Lambda S_{\mathrm{u}} - F_I I_{\mathrm{u}} + \omega I_{\mathrm{n}} - \gamma I_{\mathrm{u}}, && \text{(A1e)}\\
dI_{\mathrm{n}}/dt &= \Lambda S_{\mathrm{n}} + (1-p_I) F_I I_{\mathrm{u}} - \omega I_{\mathrm{n}} - \gamma I_{\mathrm{n}}, && \text{(A1f)}\\
dI_{\mathrm{p}}/dt &= \Lambda S_{\mathrm{p}} + p_I F_I I_{\mathrm{u}} - \omega I_{\mathrm{p}} - \gamma I_{\mathrm{p}}, && \text{(A1g)}\\
dI_{\mathrm{c}}/dt &= \Lambda S_{\mathrm{c}} + \omega I_{\mathrm{p}} - \gamma I_{\mathrm{c}}, && \text{(A1h)}\\
dR_{\mathrm{u}}/dt &= \gamma I_{\mathrm{u}} - F_R R_{\mathrm{u}} + \omega R_{\mathrm{n}}, && \text{(A1i)}\\
dR_{\mathrm{n}}/dt &= \gamma I_{\mathrm{n}} + (1-p_R) F_R R_{\mathrm{u}} - \omega R_{\mathrm{n}}, && \text{(A1j)}\\
dR_{\mathrm{p}}/dt &= \gamma I_{\mathrm{p}} + p_R F_R R_{\mathrm{u}} - \omega R_{\mathrm{p}}, && \text{(A1k)}\\
dR_{\mathrm{c}}/dt &= \gamma I_{\mathrm{c}} + \omega R_{\mathrm{p}}, && \text{(A1l)}\\
dN/dt &= \omega(S_{\mathrm{n}} + I_{\mathrm{n}} + R_{\mathrm{n}}), && \text{(A1m)}\\
dP/dt &= \omega(I_{\mathrm{p}} + R_{\mathrm{p}}), && \text{(A1n)}
\end{aligned}
$$

where parameters are specified in Table 1. The next generation matrix for this model is $G = FV^{-1}$, where matrix F represents the inflow of new infection to the infected compartments and matrix V represents the flow in the infected compartments when the population is totally susceptible. Matrices F and V are [**Ali:** *all* S_{u}&S_{n} *should be* S^*_{u}&S^*_{n}]

$$
F = \beta/N_0 \begin{bmatrix} S_{\mathrm{u}} & \eta_{\mathrm{w}} S_{\mathrm{u}} & \eta_{\mathrm{w}} S_{\mathrm{u}} & \eta_{\mathrm{c}} S_{\mathrm{u}} \\ S_{\mathrm{n}} & \eta_{\mathrm{w}} S_{\mathrm{n}} & \eta_{\mathrm{w}} S_{\mathrm{n}} & \eta_{\mathrm{c}} S_{\mathrm{n}} \\ 0 & 0 & 0 & 0 \\ 0 & 0 & 0 & 0 \end{bmatrix}, \tag{A2}
$$

$$
V = \begin{bmatrix} F_I + \gamma & -\omega & 0 & 0 \\ -(1-p_I)F_I & \omega + \gamma & 0 & 0 \\ -p_I F_I & 0 & \omega + \gamma & 0 \\ 0 & 0 & -\omega & \gamma \end{bmatrix}, \text{thus} \tag{A3}
$$

$$
V^{-1} = \begin{bmatrix} \frac{\omega+\gamma}{\omega\gamma+\gamma F_I+\gamma^2+\omega F_I p_I} & \frac{\omega}{\omega\gamma+\gamma F_I+\gamma^2+\omega F_I p_I} & 0 & 0 \\ \frac{(1-p_I)F_I}{\omega\gamma+\gamma F_I+\gamma^2+\omega F_I p_I} & \frac{F_I+\gamma}{\omega\gamma+\gamma F_I+\gamma^2+\omega F_I p_I} & 0 & 0 \\ \frac{p_I F_I}{\omega\gamma+\gamma F_I+\gamma^2+\omega F_I p_I} & \frac{\omega p_I F_I}{(\omega\gamma+\gamma F_I+\gamma^2+\omega F_I p_I)(\omega+\gamma)} & \frac{1}{\omega+\gamma} & 0 \\ \frac{\omega F_I p_I}{(\omega\gamma+\gamma F_I+\gamma^2+\omega F_I p_I)\gamma} & \frac{\omega^2 F_I p_I}{(\omega\gamma+\gamma F_I+\gamma^2+\omega F_I p_I)(\omega+\gamma)\gamma} & \frac{\omega}{(\omega+\gamma)\gamma} & \frac{1}{\gamma} \end{bmatrix}. \tag{A4}
$$

The particular form of F with two rows of zeros at the bottom, simplifies G as

$$
G = \begin{bmatrix} G_{11} & G_{12} \\ 0 & 0 \end{bmatrix}, \text{ where } G_{11} = \frac{\beta}{\gamma} C \begin{bmatrix} A S_{\mathrm{u}} & B S_{\mathrm{u}} \\ A S_{\mathrm{n}} & B S_{\mathrm{n}} \end{bmatrix}, \tag{A5}
$$

with expressions A, B and C are specified in (5). The block matrix G_{12} does not influence $\mathcal{R}_0$ (defined as the spectral radius of G). All that matters here are the eigenvalues of G_{11}, which are 0 and $\mathcal{R}_0$ (4). Also note that, all $S_{\rm u}$'s and $S_{\rm n}$'s are evaluated at the DFE (3) in matrix F (A2) and the block matrix G_{11} (A5).

5.2 On Testing Rate and Numerical Singularity

In this work, we didn't do any numerical solutions for the trajectories in our analysis. However, if one tries to do so there would be a singularity issue to deal with. Specifically, the numerical singularity issue with the chosen σ (1) is that the population in S compartments appeared to blow up when the DFE is achieved. This is once the only untested people are susceptibles, the FOI will become $\Lambda = 0$, testing rate $F_s = \rho N_0/S_{\rm u}$. Thus, the first equation of the model (A1) will become $dS_{\rm u}/dt = -\rho N_0 + \omega S_{\rm n}$. Thus changes in $S_{\rm u}$ will be no longer dependent on $S_{\rm u}$ with a linear rate of leaving the $S_{\rm u}$ compartment. IN fact the testing rate, σ, should be formulated such that people from the untested compartments will not be tested if they are not there. One way to fix this issue, is to consider a maximum testing rate, τ (1/day). In general, we want to test at a rate of ρ across the whole population. This won't always be possible, so we impose a maximum rate of τ per testable person and redefine $\sigma = \frac{\tau\rho N_0}{\tau W + \rho N_0}$, with the assumption that $\tau \gg \rho$. This alteration in σ, does not change any results related to $\mathcal{R}_0$, thus we only impose it in the simulation of the epidemic dynamic.

5.3 Taylor Approximation of $\mathcal{R}_0$ at $\rho = 0$

The basic reproduction number, $\mathcal{R}_0$, close to $\rho = 0$ can be approximated linearly in ρ by using Taylor approximation. it follows

$$\mathcal{R}_0 \approx \beta/\gamma + \frac{\beta\rho}{\omega(\omega+\gamma)\gamma^2 W_S}\Big(\gamma(\eta_{\rm w}-1)(\gamma W_S + \omega W_I) + (\eta_{\rm c}-1)P_i W_i \omega^2\Big) + \mathcal{O}(\rho^2). \quad \text{(A6)}$$

Also, to analyze the influence of ω on $\mathcal{R}_0$, the approximation (A6) was used. Then it is straight forward to have

$$\partial\mathcal{R}_0/\partial\omega = \frac{-\beta\rho}{\gamma W_S \omega^2(\gamma+\omega)^2}(a\omega^2 + b\omega + c), \quad \text{(A7)}$$

where $a = (\eta_{\rm w}-1)W_I - (\eta_{\rm c}-1)P_I W_I = ((s-p_I)\eta_{\rm c} + (p_I-1))W_I$, $b = 2(\eta_{\rm w}-1)\gamma W_S$ and $c = (\eta_{\rm w}-1)\gamma^2 W_S$. Given that $0 \le \eta_{\rm c} \le \eta_{\rm w} \le 1$, one can easily derive $b \le 0$ and $c \le 0$.

Note that in general, the necessary and sufficient condition for $a \ge 0$ is $(s-p_I)\eta_{\rm c} \ge (1-p_I)$, where $s = \frac{\eta_{\rm w}}{\eta_{\rm c}} \ge 1$.

In the case of "perfect isolation", i.e., when $\eta_{\rm w} = 0$ and consequently $\eta_{\rm c} = 0$, it is straightforward to see that $a \le 0$, $b < 0$ and $c < 0$. Thus, $\partial\mathcal{R}_0/\partial\omega \ge 0$. As an example, in the case of a very accurate testing regime, i.e., $P_I = 1$, $a \ge 0$ is achieved. If $a \ge 0$, the quadratic expression in (A7), has Real roots. Assuming that $\omega_1 < 0$ and $\omega_2 > 0$ be the roots of the quadratic expression in $\partial\mathcal{R}_0/\partial\omega$. Thus, $\partial\mathcal{R}_0/\partial\omega > 0$ for $0 < \omega < \omega_2$ and $\partial\mathcal{R}_0/\partial\omega < 0$ for $\omega > \omega_2$.

5.4 rate of returning tests

[**Ali:** *needs editig*] The linearization of $\mathcal{R}_0$ around $\rho = 0$ is

$$\mathcal{R}_0 \approx \beta/\gamma + \frac{\beta\rho}{\omega(\omega+\gamma)\gamma^2 W_s}\Big(\gamma(\eta_w - 1)(\gamma W_s + \omega W_i) + (\eta_c - 1)P_i W_i \omega^2\Big). \tag{A8}$$

So when $\rho \approx 0$ we have

$$\partial\mathcal{R}_0/\partial\omega \approx \frac{-\beta\rho}{\gamma W_s \omega^2(\gamma+\omega)^2}(a\omega^2 + b\omega + c),$$

where $a = (\eta_w - 1)W_i - (\eta_c - 1)P_i W_i$, $b = 2(\eta_w - 1)\gamma W_s$ and $c = (\eta_w - 1)\gamma^2 W_s$.

Perhaps counter-intuitively, the equation above does not predict that $\mathcal{R}_0$ is monotone decreasing with respect to ω. In other words; our model does not predict that returning test results more rapidly *always* lower $\mathcal{R}_0$. In order to gain insight into this intriguing behavior, we examine the zeroes of $\frac{\partial\mathcal{R}_0}{\partial\omega}(\omega)$. Defining the following quantity, Q, will help us write the roots of $\partial\mathcal{R}_0/\partial\omega$ neatly as follows.

$$Q = \frac{W_i}{W_s}\left(1 - \frac{n_t - 1}{n_w - 1}P_i\right). \tag{A9}$$

With that in mind, we can write the roots of $\partial\mathcal{R}_0/\partial\omega$ as

$$\omega_1 = \frac{\gamma}{-\sqrt{1-Q} - 1} \tag{A10}$$

$$\omega_2 = \frac{\gamma}{\sqrt{1-Q} - 1}. \tag{A11}$$

Note that the zeroes are real if and only if $Q < 1$. Note that have $\eta_c < \eta_w$, so if $P_i \approx 1$, we will have $Q < 0 < 1$. Thus, if we assume near-perfect test sensitivity, ω_1 and ω_2 will be real.

Assuming ω_1, ω_2 are real, it is easy to confirm that $\omega_1 < 0$ by looking at the denominator. To see that $\omega_2 > 0$, recall that $Q < 0$, so $\sqrt{1-Q} > 1$ and so $\sqrt{1-Q} - 1 > 0$. Knowing that $\omega_1 < 0$, the only root of interest (i.e., biologically relevant quantity) is ω_2.

We can prove that $\partial\mathcal{R}_0/\partial\omega > 0$ when $\omega \in (0, \omega_2)$ and $\partial\mathcal{R}_0/\partial\omega < 0$ when $\omega \in (\omega_2, \infty)$ by computing the limits of $\partial\mathcal{R}_0/\partial\omega$ at 0 and ∞ respectively. So it follows that $\mathcal{R}_0$ has a global maximum with respect to ω at $\omega = \omega_2$.

Now we want to characterize the parameter regions on which $\partial\mathcal{R}_0/\partial\omega < 0$ (i.e., the conditions under which returning test results more rapidly is favorable). By the previous analysis, this is equivalent to solving for $\omega > \omega_2$. So

$$\omega > \omega_2$$

$$\omega > \frac{\gamma}{\sqrt{1-Q} - 1}$$

$$\sqrt{1-Q} > \frac{\gamma}{\omega} + 1 \tag{A12}$$

$$1 - Q > (\frac{\gamma}{\omega} + 1)^2. \tag{A13}$$

Substituting in Q from (A9) we have

$$1 - \frac{W_i}{W_s}\left(1 - \frac{n_t - 1}{n_\omega - 1}P_i\right) > \left(\frac{\gamma}{\omega} + 1\right)^2 \tag{A14}$$

$$-\frac{W_i}{W_s}\left(1 - \frac{n_t - 1}{n_\omega - 1}P_i\right) > \left(\frac{\gamma}{\omega} + 1\right)^2 + 1 \tag{A15}$$

$$\frac{W_i}{W_s}\left(\frac{1 - n_t}{1 - n_\omega}P_i - 1\right) > \left(\frac{\gamma}{\omega} + 1\right)^2 + 1. \tag{A16}$$

Since all steps in deriving (A16) are reversible, (A16) gives a necessary and sufficient condition for $\omega > \omega_2$, which characterizes when returning tests more rapidly would cause a decrease in $\mathcal{R}_0$.

5.5 Expensive vs. cheap tests

The use of tests cheaper than RT-PCR has been proposed as a potential strategy for containing the COVID-19 pandemic. While cheaper tests may be less sensitive and reliable than RT-PCR, they allow for broader and more intense testing. In the analysis below, we compare the $\mathcal{R}_0$ predicted by our model depending on the testing strategy.

Consider a test that allows us to test at rate ρ_1 and has sensitivity $P_{i,1}$, and another test that allows us to test at ρ_2 and has sensitivity $P_{i,2}$. Suppose that $\rho_1 > \rho_2$. Recall that the linearization of $\mathcal{R}_0$ around $\rho \approx 0$ is given by

$$\mathcal{R}_0 \approx \beta/\gamma + \frac{\beta\rho}{\omega(\omega+\gamma)\gamma^2 W_s}\Big(\gamma(\eta_{\mathrm{w}} - 1)(\gamma W_s + \omega W_i) + (\eta_{\mathrm{c}} - 1)P_i W_i \omega^2\Big).$$

Treating $\mathcal{R}_0$ as a function of ρ and P_i,we can reduce the inequality

$$\mathcal{R}_0(\rho_2, P_{i,2}) < \mathcal{R}_0(\rho_1, P_{i,1})$$

into

$$\rho_1\left(\gamma(\eta_{\mathrm{w}} - 1)(\gamma W_s + \omega W_i) + (\eta_{\mathrm{c}} - 1)P_{i,1}W_i\omega^2\right) - \rho_2\left(\gamma(\eta_{\mathrm{w}} - 1)(\gamma W_s + \omega W_i) + (\eta_{\mathrm{c}} - 1)P_{i,2}W_i\omega^2\right) > 0$$

$$\vdots$$

$$\frac{\rho_2 P_{i,2} - \rho_1 P_{i,1}}{\rho_1 - \rho_2} > \frac{1 - \eta_{\mathrm{w}}}{1 - \eta_{\mathrm{c}}} \cdot \frac{\gamma(\gamma W_s + \omega W_i)}{\omega^2 W_i} \tag{A17}$$

Note that the RHS is positive, thus a necessary condition for the inequality above to hold is that $\rho_2 P_{i,2} > \rho_1 P_{i,1}$, equivalently

$$\frac{P_{i,2}}{P_{i,1}} > \frac{\rho_1}{\rho_2}. \tag{A18}$$

To state an example of this, if test A is three times as expensive as test B (and hence one can test three times as many people with test B), using test A rather than B will be favorable only if test A is at least 3 times more sensitive than test B. Note that this is a

necessary but not sufficient condition, so even if test A is three times more sensitive, it is still possible for test B to be more effective.

Eq. (A17) tells us precisely when a test corresponding to $\rho_2, P_{i,2}$ will yield a lower $\mathcal{R}_0$ than a test corresponding to $\rho_1, P_{i,1}$, where $\rho_1 > \rho_2$. Some of the qualitative *trends* that favor test 2 (the higher-sensitivity test) include

- individuals who test positive self-isolate much more than individuals who are waiting for their test result.
- the time it takes to return tests is much shorter than the mean infectious period.
- the testing intensity is much greater for infected individuals than susceptible individuals.

5.6 Literature Review

5.6.1 Explicit models of TTI (trace/test/isolate) based on network or agent-based models

(Endo et al., 2020) [**Ali:** *It seems to me that this is just a statistical model to estimate the parent-offspring of an infected index, not sure if it fits into agent-based group!*] Used simulation on a branching process model to assess the forward and backward contact tracing efficiency. Assuming a negative-binomial branching process with a mean R, reproduction number, and overdispersion parameter k, the mean total number of generation G3 and averted G3 are estimated. The effectiveness of TTI is defined as the ratio of averted to the mean.

(Jenness et al., 2020) developed a network-based transmission model for SARS-CoV-2 on the Diamond Princess outbreak to characterize transmission dynamics and to estimate the epidemiological impact of outbreak control and prevention measures.

(Elbanna et al., 2020) [seems similar to MacPan model!]

(de Celles et al., 2020) Was discussed in the Math 747 SEIR Asymptomatic and symptomatic I_1, I_2. Used linear chain trick Stringency index as a control force lowering β.

(Rice et al., 2020) Effect of school closures on mortality. Reproduce Report 9 results by spatial agent based CovidSim.

5.6.2 Models of repeated random testing of isolated populations

Bergstrom et al. (2020) (1) Model, assumptions: They developed a function, namely expected exposure $E(C, \tau)$, to approximate trade-offs between the frequency of testing, n, the sensitivity of testing, q, and the delay between testing and results, d. This function is explicitly derived and was connected the effective reproduction number $R = \mathcal{R}_0 S$, where S is the proportion of population susceptible. assumption that transmission rates are a step function: individuals who have COVID-19 go from non-infectious to fully infectious instantaneously, and remain fully infectious until they are no longer able to transmit disease. Test sensitivity takes the same form over the course of infection. More sophisticated models could allow varying infectiousness and varying sensitivity over time, as in (Larremore et al., 2020).

(Lopman et al., 2020) Used a Deterministic SEIR model, incorporated TTI, applicable to a university setting. They assumed a fairly high reproductive number that is not reduced through social distancing measures. They found that community-introduction of SARS-CoV-2 infection onto campus can be relatively controlled with effective testing, isolation, contract tracing and quarantine.

(Tuite et al., 2020) used an age-structured compartmental model of COVID-19 transmission in the population of Ontario, Canada. We compared a base case with limited testing, isolation and quarantine to different scenarios.

5.6.3 Other maybe-related works

(Arino and Portet, 2020) developed a SLIAR compartmental model to study the spread of an epidemic, specifically COVID, in a population. The model incorporates an Erlang distribution of times of sojourn in incubating, symptomatically and asymptomatically infectious compartments. Basic reproduction number is derived. Also, sensitivity analysis with respect to the underlying parameters for the following two outputs was carried out; (i) the number of observable cases during the course of the epidemic and at the peak, and (ii) the timing of the peak of the outbreak. Sensitivity analysis is performed using the R package multisensi.

(Ruszkiewicz et al., 2020) novel with-in-a-minute breath testing with 80% accuracy.